RESEARCH ARTICLE

Structure Prediction and Binding Site Analysis of Human Sperm Hyaluronidases

Prasanth Gunasekaran[1], Madhukar Hemamalini[2], Rajakannan Venkatachalam[3]

Abstract

Background: Sperm cell hyaluronidases are important class of enzymes which plays a prominent role in hydrolysing hyaluronan during sperm penetration through the layer of cumulus and zona pellucida of egg. Clinically sperm hyaluronidases play important role in analysing sperm binding quality during IVF treatments Hyaluronan Binding Assay. The functions of sperm hyaluronidases such as penetrating the hyaluronan matrix of cumulus layer, inducing hyaluronan based acrosome reaction were directly related to substrate binding efficiency of these enzymes. Though hyaluronidases were confirmed to play the hyaluronan hydrolysing role in fertilization, there is no structural evidence to prove their difference in molecular weight-based substrate specificity and their multifunctional activity in fertilization. This work presents the evidence on the binding modes of hyaluronan with sperm cell hyaluronidases using homology modelling and molecular docking methods.

Methods: The different isoforms of human sperm hyaluronidases were modelled using human hyaluronidase 1 (PDB code 2PE4) and the optimized structure of hyaluronan from the crystal structure of bee venom hyaluronidase complexed with HA tetramer (PDB Code: 1vcz) was docked using AUTODOCK TOOLS. The results are evaluated based on the complex binding energy and interaction with substrate binding residues.

Results: The molecular docking results confirms the binding of hyaluronan with HYAL-2 in the deep substrate binding groove, which was absent in HYAL-3 and HPH-20 hyaluronan complex. The binding of hyaluronan with HPH-20 and HYAL-3, involved in neutral-active domain and residues present in perpendicular beta sheets. The binding mode of HYAL-2 is more on acid-active region of the enzyme which was considered to induce hyaluronan dependent cell signalling and AR activation.

Conclusion: The results concludes that the substrate accommodation pattern of HYAL-2 was differed from HYAL-3 and HPH-20 where the acid active domain of HYAL-2 of may predominantly involves in AR activation and zona pellucida penetration apart from cumulus HA degradation.

Keywords: Acrosome reaction, Homology modeling, Hyaluronic acid binding, Molecular docking, Sperm hyaluronidases.

International Journal of Infertility and Fetal Medicine (2022): 10.5005/jp-journals-10016-1280

Introduction

Hyaluronidases present in sperm cells are endo-N-acetyl hexosaminidases (EC 3.2.1.35) which hydrolyze the polysaccharide HA into tetra saccharides HA during the fertilization process. The glycosylphosphatidylinositol (GPI) anchored sperm hyaluronidases present on the sperm surface specifically act on the cumulus layer and initiate the AR. Followed by this process, the soluble hyaluronidases and acrosomal proteins clear the zona pellucida layer of the ovum to reach the plasma membrane of the oocyte. In humans HYAL-2, HYAL-3, and HPH-20 are membrane-anchored proteins whose anchors can be cleaved to produce soluble enzyme isoforms. The HPH-20 or sperm adhesion molecule 1 (SPAM1) is a ~57 kDa GPI-linked protein that was the first identified sperm hyaluronidase believed to participate in sperm-egg fusion and act on HA polysaccharides.[1] The *in vitro* research on the function of hyaluronidases shows that with the aid of HYAL-2, the HPH-20 is expected to cleave high molecular weight HA polysaccharide present in the cumulus layer to produce 20 kDa HA polysaccharide, where the HYAL-2 is a ~53 kDa acid active hyaluronidase predominantly presents in acrosome and inner acrosomal membrane of sperm.[2] Finally, the HYAL-3 is a ~46 kDa acid-active hyaluronidase that prominently participates in hydrolyzing the 20 kDa HA together with HPH-20 and HYAL-2 to form the final product in the cumulus oophorous penetration process. The HYAL-3 is expected to play an important role in zona pellucida penetration and AR induction through HA signaling.[3] Since all three hyaluronidases show more than 40% sequence identity and similar function, these enzymes were considered to play redundant parts with one another. Since the evidence on the functions of the three hyaluronidases was not enough to establish their exact function in hydrolyzing different molecular weight HA, we need molecular and structural based evidence to conclude their differences in molecular weight-based substrate specificity.[4,5]

[1,3]Centre of Advanced Study in Crystallography and Biophysics, University of Madras, Guindy Campus, Chennai, Tamil Nadu, India

[2]Department of Chemistry, Mother Teresa Women's University, Kodaikanal, Tamil Nadu, India

Corresponding Author: Rajakannan Venkatachalam, Centre of Advanced Study in Crystallography and Biophysics, University of Madras, Guindy Campus, Chennai, Tamil Nadu, India, Phone: +91 9566100017, e-mail: gnrphipsi@gmail.com

How to cite this article: Gunasekaran P, Hemamalini M, Venkatachalam R. Structure Prediction and Binding Site Analysis of Human Sperm Hyaluronidases. Int J Infertil Fetal Med 2022;xx(xx):1–5.

Source of support: Nil

Conflict of interest: None

Materials and Methods

The amino sequence files of hyaluronidases were downloaded from the protein sequence database UniProt[6] and the sequences were analyzed using the National Center for Biotechnology Information protein basic local alignment search tool server[7] to identify the sequence identity of hyaluronidases with one another. The data such as UniProt accession number, protein name,

Table 1: Results from sequence alignment, structure alignment, and molecular docking of sperm hyaluronidases with HA

Name	*HPH-20*	*HYAL-2*	*HYAL-3*
Uniprot ID	P38567	Q12891	O43820
Amino acids	509	473	417
Gene	SPAM1	HYAL-2	HYAL-3
Sequence identity with HYAL-1	42.82%	43.56%	44.76%
Molecular weight	~57 kDa	~53 kDa	~46 kDa
Amino acids involved in hydrogen bonds with HA	TYR 219, ARG 305, TYR 264, TYR 92, ASN 54, THR 89, ASP 146, TRP 147	ILE 326, THR 294, VAL 292, TYR 291, PHE 293, TYR 253, ARG 271, LEU 207, ASP 41	PHE 73, ASN 36, TYR 200, ARG 290, GLU 129, ASN 36

number of amino acids in the protein, and the molecular weight of hyaluronidases were tabulated (Table 1). The downloaded sequences were aligned using Multalin sequence alignment server[8] and to obtain the structure of sperm cell hyaluronidases, the three-dimensional coordinates of human HYAL-1 involved in tumor growth and angiogenesis (PDB: 2PE4)[9] were used. The structure was modeled, and energy was minimized in the molecular modeling server Swiss model and validated by the Ramachandran plot.[10–15] The HA was docked with modeled sperm cell hyaluronidases using AutoDock tools 4.2,[16] where the HA tetramer was obtained from the BVHYAL-hyaluronan complex (PDB: 1VCZ).[17] The grid box dimensions of HYAL-2–HA docking are set to 52 × 38 × 40 with 0.375Å spacing centered to 43.416, –24.930, and –14.009, and the grid box dimensions for HPH-20-HA docking were 50 × 42 × 50 with 0.375Å spacing centered to 41.875, –24.852, and –15.296. The grid box dimensions for HA with HYAL-3 were 40 × 40 × 58 with 0.375 Å spacing centered to 41.215, –25.941, and –14.994 for all three hyaluronidase-HA dockings the grid box parameters were adjusted to cover essential active site regions in substrate binding groove. A genetic algorithm was chosen with 10 runs for search parameters, and Lamarckian GA was chosen to get the final output. The results from the docking were analyzed for HA interactions with modeled structures using PyMOL.[18]

Results and Discussion

Sequence Alignment

Sequence alignment of HPH-20 with HYAL-2 and HYAL-3 shows ~40% overall sequence identity for HPH-20 with HYAL-2 and ~37% overall sequence identity for HPH-20 with HYAL-3 (Fig. 1) where sequence alignment of HYAL-2 with HYAL-3 show ~42% identity with many conserved residues in the HA binding regions. Since HPH-20 is both a neutral and acid-active enzyme, it has two domains for hyaluronidase activity called peptide-1 domain for neutral pH hyaluronidase activity and peptide-3 for acid pH hyaluronidase activity. Sequence alignment for these specific domains shows that the acid-active domain (peptide-3) of HPH-20 has ~75% sequence identity with HYAL-2 acid-active domain and ~58% sequence identity with HYAL-3 acid-active domain, but for a neutral-active domain, the HYAL-3 shows 75% sequence identity and HYAL-2 has ~67.74% sequence identity with HPH-20 neutral active domain. Other than peptide-1 and peptide-2 regions, there is a specific domain called peptide-2 which is considered to play important role in HA-induced cell signaling, this specific domain in HPH-20 has a sequence identity of ~45% with HYAL-3 and ~70% with HYAL-2. From these results, the maximum sequence identity of HYAL-2 with HPH-20 in the acid-active domain shows there their involvement in zona pellucida penetration with high molecular weight substrate binding. The maximum sequence identity of a neutral-active domain of HYAL-3 with HPH-20 shows its abundance in the plasma membrane with involvement in cumulus penetration.

Structure Modeling and Structure Alignment

The sperm hyaluronidase structures were modeled using the human HYAL-1 crystal structure (PDB: 2PE4), three hyaluronidases show ~40–43% sequence identity, and modeled structures were validated through the Ramachandran plot. The modeled structure of HPH-20 has 91.73% present in favored region of the Ramachandran plot, and the modeled structures of HYAL-2 occupy 93.40% of favored region in the Ramachandran plot.[19] From all HYAL-3 structure has its maximum structure of 93.73% in favored regions of the Ramachandran plot. The modeled structures have ~0.067Å RMSD deviation from the crystal structure of HYAL-1 and ~0.103Å RMSD between three modeled structures aligned (Fig. 2) where there is a maximum structure difference in the C-terminal region. The 364–439 amino acids of C-terminal regions in HYAL-3 differ from the other two modeled structures by the presence of a long loop extended and ended by an antiparallel ß-sheet. The same C-terminal regions have two antiparallel ß-sheets with a small helix portion in HYAL-2 and HPH-20 (Fig. 2). In the conserved binding groove, the HYAl-2 has an ß-sheet structure, but in HYAL-3 and HPH-20, this region has a loop structure. Like the binding groove, the secondary structure of peptide-2 in HYAL-2 has a small turn, but this region in HPH-20 and HYAL-3 has a continuous loop structure and in the peptide-3 region where the acid-activity is shown, the HYAL-2 has differed with the presence of continues loop (HYAL-3 and HPH-20 has small turn).[20–22]

Molecular Docking

The molecular docking of HA from the BVHYAL crystal structure with sperm hyaluronidases shows that the residues involved in interaction with HA in HPH-20 were mostly from both the side of the binding groove and the ligand make hydrogen bonds with residues Y264, R305, N54, T89, Y219, W147, D146, and Y92 (Figs 3 and 4). The molecular docking of HA with HYAL-2 results that the HA binds inner region of the binding groove where most of the residue is present in peptide-1 and peptide-2 with one residue in the peptide-3 region. The HA makes hydrogen bonds with residues D41, I326, F293, T294, Y253, L207, R271, and Y291 (Figs 3 and 4). Like HYAL-2, HA binds mostly with the peptide-2 region, but the difference is the involvement of many residues from the loops connecting peptide -3 (Figs 3 and 4). The docking results show that the tetramer buried itself deep in the HYAL-2 binding groove, but in HYAL-3 and HPH-20, it interacts mostly with residues present in perpendicular ß-sheets and the peptide-1 region of the binding groove. On analyzing the docking results, the binding mode of HYAL-2 is more on acid-active region and region which considered inducing HA bases cell signaling and

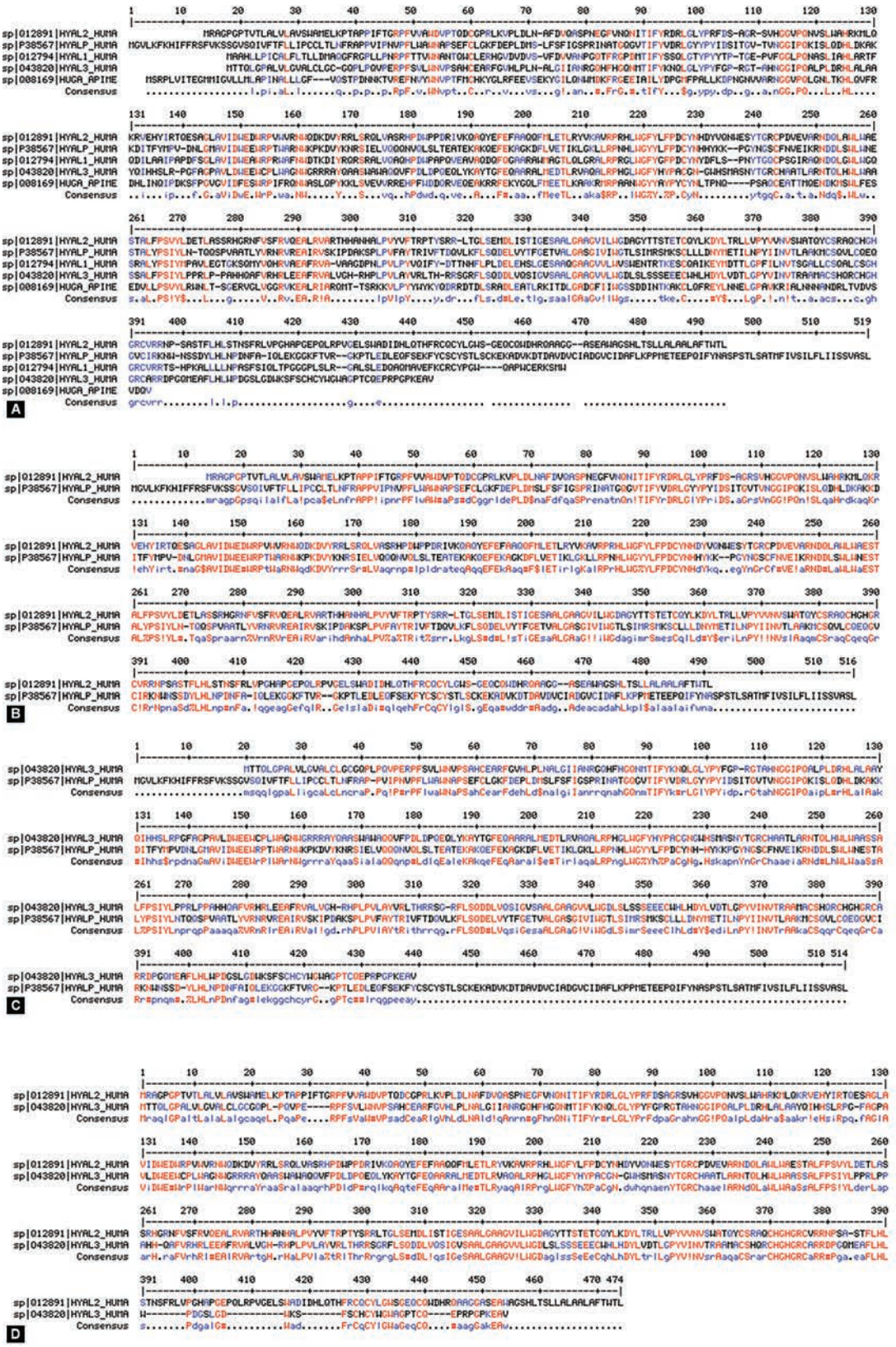

Figs 1A to D: (A) Sequence alignment of human sperm hyaluronidases with bee venom hyaluronidase and human hyaluronidase-1 where blue regions are partially conserved amino acids and red regions are completely conserved amino acids; (B) Sequence alignment of human HPH-20 with human HYAL-2; (C) Sequence alignment of human HPH-20 with human HYAL-3; (D) Sequence alignment of human HYAL-2 with human HYAL-3 having ~42% sequence identity where blue regions are partially conserved amino acids and red regions are completely conserved amino acids

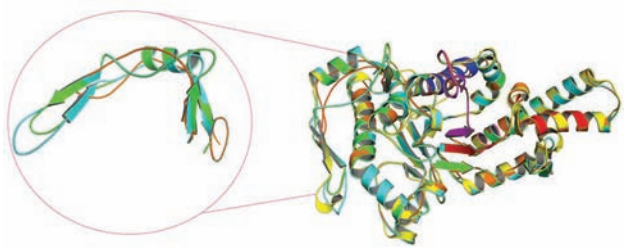

Fig. 2: Structure alignment of modeled structures of HPH-20, HYAL-2, HYAL-3 (HYAL-3: orange, HPH-20: green, HYAL-2: cyan. Peptide-1: blue, Peptide-2: magenta, Peptide-3: blue) and back view of C-terminal regions of HPH-20, HYAL-2, and HYAL-3 showing the difference in secondary structure by the presence of loop in HYAL-3 structure when compared with HYAL-2 and HPH-20 (HYAL-3: orange, HPH-20: green, HYAL-2: cyan) (zoomed inside the sphere in left)

AR activation, but for HPH-20 and HYAL-3, more residues involved in HA binding were neutral-active domain and residues present in perpendicular ß-sheets.[23,24]

Hyaluronidase Specificity based on the Results

The molecular docking results, it confirms the binding of hyaluronan with HYAL-2 in the deep substrate binding groove, but this mode of binding is not seen in HYAL-3 and HPH-20. Further, to differentiate the morphological information of defective head and normal head, tests such as computer-assisted sperm analysis and HBA will be performed in the future. The HBA analysis will give the critical analysis of hyaluronidase lacking sperm cell activity, where less penetration with the artificial hyaluronan layer indicates the absence of hyaluronan hydrolyzing enzyme (hyaluronidase) in the sperm cells.[25,26]

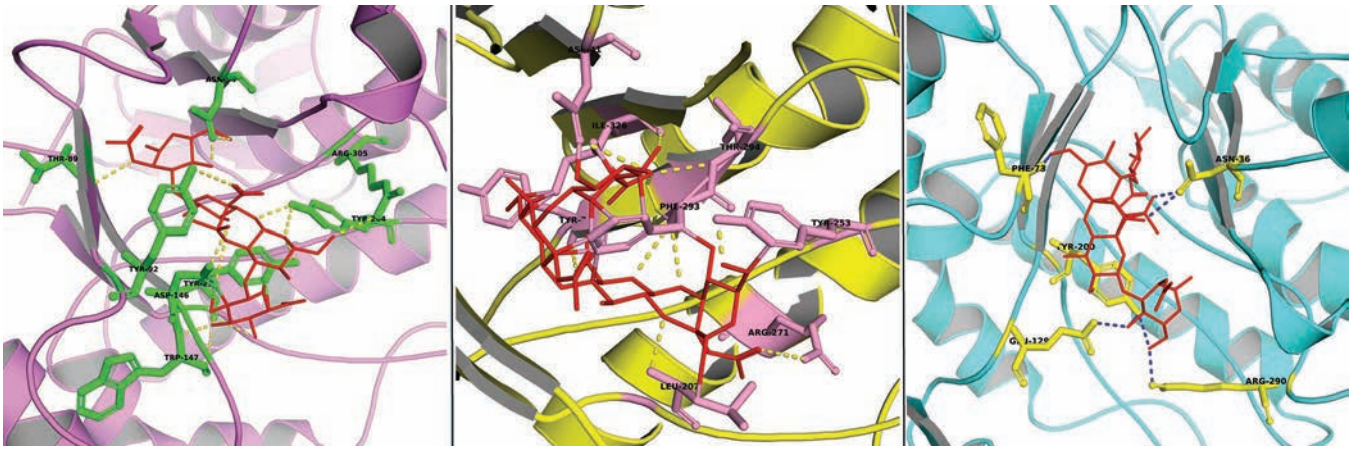

Fig. 3: Cartoon representation of the interaction between HA (red dark line representation) and binding sites of HPH-20 (pink cartoon), HYAL-2 (yellow cartoon), and HYAL-3 (cyan cartoon), where the amino acids in binding regions were represented as sticks

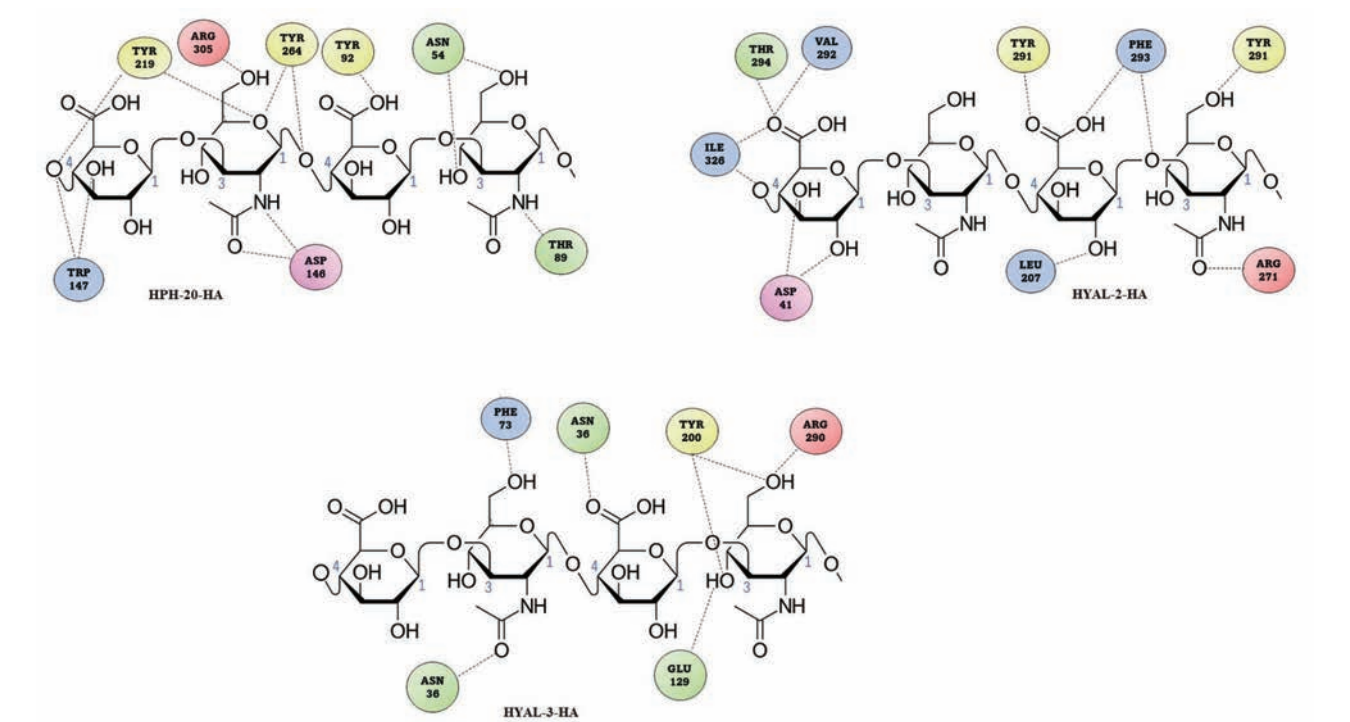

Fig. 4: Two-dimensional representation of the interaction of amino acids from hyaluronidases to the HA tetramer (from left to right: HPH-20, HYAL-2, and HYAL-3)

Conclusion

The maximum identity of active site regions of the HPH-20 and HYAL-2 shows that the HYAL-2 and HPH-20 may be the important acid-active hyaluronidases that participate in high molecular weight substrate recognition and degradation. The result of molecular docking shows that there was a prominent difference in HA binding with HYAL-2 compared to the binding mode of HPH-20 and HYAL-3, which concludes that the HYAL-2 acid-active domain may predominantly be involved in AR activation and zona pellucida penetration apart from cumulus HA degradation.

Reference

1. Cherr GN, Yudin AI, Overstreet JW. The dual functions of GPI-anchored PH-20: hyaluronidase and intracellular signaling. Matrix Biol 2001;20(8):515–525. DOI:10.1016/s0945-053x(01)00171-8
2. Modelski MJ, Menlah G, Wang Y, et al. Hyaluronidase 2: a novel germ cell hyaluronidase with epididymal expression and functional roles in mammalian sperm. Biol Reprod 2014;91(5):109. DOI: 10.1095/biolreprod.113.115857
3. Reese KL, Aravindan RG, Griffiths GS, et al. Acidic hyaluronidase activity is present in mouse sperm and is reduced in the absence of SPAM1: evidence for a role for hyaluronidase 3 in mouse and human sperm. Mol Reprod Dev 2010;77(9):759–772. DOI: 10.1002/mrd.21217
4. Esterhuizen AD, Franken DR, Bosman E, et al. Relationship between human spermatozoa-hyaluronan-binding assay, conventional semen parameters and fertilisation rates in intracytoplasmic spermatozoa injection. Andrologia 2015;47(7):759–764. DOI: 10.1111/and.12326
5. Lazarevic J, Wikarczuk M, Somkuti SG, et al. Hyaluronan binding assay (HBA) vs. sperm penetration assay (SPA): Can HBA replace the SPA test in male partner screening before in vitro fertilization? J Exp Clin Assist Reprod 2010;7:2. DOI: 10.1016/j.fertnstert.2007.07.1254
6. UniProt Consortium. UniProt: a worldwide hub of protein knowledge. Nucleic Acids Res 2019;47(D1):D506–D515. DOI: 10.1093/nar/gky1049
7. Altschul SF, Gish W, Miller W, et al. Basic local alignment search tool. J Mol Biol 1990;215(3):403–410. DOI: 10.1016/S0022-2836(05)80360-2
8. Corpet F. Multiple sequence alignment with hierarchical clustering. Nucleic Acids Res 1988;16(22):10881–10890. DOI:10.1093/nar/16.22.10881
9. Chao KL, Muthukumar L, Herzberg O. Structure of human hyaluronidase-1, a hyaluronan hydrolyzing enzyme involved in tumor growth and angiogenesis. Biochemistry 2007;46(23):6911–6920. DOI: 10.1021/bi700382g
10. Waterhouse A, Bertoni M, Bienert S, et al. SWISS-MODEL: homology modelling of protein structures and complexes. Nucleic Acids Res 2018;46(W1):W296–W303. DOI: 10.1093/nar/gky427
11. Bienert S, Waterhouse A, de Beer TAP, et al. The SWISS-MODEL Repository-new features and functionality. Nucleic Acids Res 2017;45(D1):D313–D319, DOI: 10.1093/nar/gkw1132
12. Guex N, Peitsch MC, Schwede T. Automated comparative protein structure modeling with SWISS-MODEL and Swiss-PdbViewer: a historical perspective. Electrophoresis 2009;30(1):S162–S173. DOI: 10.1002/elps.200900140
13. Studer G, Rempfer C, Waterhouse AM, et al. QMEANDisCo–distance constraints applied on model quality estimation. Bioinformatics 2020;36(6):1765–1771. DOI: 10.1093/bioinformatics/btz828
14. Benkert P, Biasini M, Schwede T. Toward the estimation of the absolute quality of individual protein structure models. Bioinformatics 2011;27(3):343–350. DOI: 10.1093/bioinformatics/btq662
15. Bertoni M, Kiefer F, Biasini M, et al. Modeling protein quaternary structure of homo-and hetero-oligomers beyond binary interactions by homology. Sci Rep 2017;7(1):1048010. DOI: 1038/s41598-017-09654-8
16. Morris GM, Huey R, Lindstrom W, et al. AutoDock4 and AutoDockTools4: automated docking with selective receptor flexibility. J Comput Chem 2009;30(16):2785–2791. DOI: 10.1002/jcc.21256
17. Marković-Housley Z, Miglierini G, Soldatova L, et al. Crystal structure of hyaluronidase, a major allergen of bee venom. Structure 2000;8(10):1025–1035. DOI: 10.1016/s0969-2126(00)00511-6
18. DeLano, W. L. (2009). The PyMOL Molecular Graphics System; DeLano Scientific: San Carlos, CA, 2002.
19. Martin-Deleon PA. Germ-cell hyaluronidases: their roles in sperm function. Int J Androl 2011;34(5 Pt 2):e306–e318. DOI: 10.1111/j.1365-2605.2010.01138.x
20. Lin Y, Mahan K, Lathrop WF, et al. A hyaluronidase activity of the sperm plasma membrane protein PH-20 enables sperm to penetrate the cumulus cell layer surrounding the egg. J Cell Biol 1994;125(5):1157–1163. DOI: 10.1083/jcb.125.5.1157
21. Meyer MF, Kreil G, Aschauer H. The soluble hyaluronidase from bull testes is a fragment of the membrane-bound PH-20 enzyme. FEBS Lett 1997;413(2):385–388. DOI: 10.1016/s0014-5793(97)00936-8
22. Botzki A, Rigden DJ, Braun S, et al. L-Ascorbic acid 6-hexadecanoate, a potent hyaluronidase inhibitor. X-ray structure and molecular modeling of enzyme-inhibitor complexes. J Biol Chem 2004;279(44):45990–45997. DOI:10.1074/jbc.M406146200
23. Zeng HJ, Yang R, You J, et al. Spectroscopic and docking studies on the binding of liquiritigenin with hyaluronidase for antiallergic mechanism. Scientifica (Cairo) 2016;2016:9178097. DOI: 10.1155/2016/9178097
24. Hunnicutt GR, Primakoff P, Myles DG. Sperm surface protein PH-20 is bifunctional: one activity is a hyaluronidase and a second, distinct activity is required in secondary sperm-zona binding. Biol Reprod 1996;55(1):80–86. DOI:10.1095/biolreprod55.1.80
25. Hunnicutt GR, Mahan K, Lathrop WF, et al. Structural relationship of sperm soluble hyaluronidase to the sperm membrane protein PH-20. Biol Reprod 1996;54(6):1343–1349. DOI:10.1095/biolreprod54.6.1343
26. Stern R, Jedrzejas MJ. Hyaluronidases: their genomics, structures, and mechanisms of action. Chem Rev 2006;106(3):818–839. DOI: 10.1021/cr050247k